Molecular Ferroelectrics

DOI: 10.1002/anie.201410523

A High-Temperature Molecular Ferroelectric Zn/Dy Complex Exhibiting Single-Ion-Magnet Behavior and Lanthanide Luminescence**

Jérôme Long, Jérôme Rouquette, Jean-Marc Thibaud, Rute A. S. Ferreira, Luís D. Carlos, Bruno Donnadieu, Veaceslav Vieru, Liviu F. Chibotaru, Leszek Konczewicz, Julien Haines, Yannick Guari, and Joulia Larionova*

Abstract: *Multifunctional molecular ferroelectrics are exciting materials synthesized using molecular chemistry concepts, which may combine a spontaneous electrical polarization, switched upon applying an electric field, with another physical property. A high-temperature ferroelectric material is presented that is based on a chiral Zn^{2+}/Dy^{3+} complex exhibiting Dy^{3+} luminescence, optical activity, and magnetism. We investigate the correlations between the electric polarization and the crystal structure as well as between the low-temperature magnetic slow relaxation and the optical properties.*

One of the recent developments of molecular chemistry which emerged in the last decade concerns the rational design of multifunctional molecule-based materials in which the targeted compounds may exhibit different physical features when subjected to various external stimuli.[1] The reason for the interest in such materials is driven not only from a strictly fundamental aspect, but also by potential technological applications in various areas such as information storage, sensors, spintronics, and biology.[2] In the scope of molecular magnetic materials, various bifunctional systems combining for example magnetic properties with optical activity,[3] nonlinear optical properties,[4] porosity,[5] chirality,[6] conductivity,[7] luminescence,[8] or ferroelectricity[9] have been reported. Such properties can simply coexist in the same crystal lattice, but cross- or synergetic effects can also be expected. Recently, breakthroughs in this field have been made by the discovery of a correlation between magnetic and luminescent properties in magneto-optical systems incorporating lanthanide ions.[10]

Molecular ferroelectrics are compounds in which the spontaneous electrical polarization may be switched upon applying an electrical field.[11] Such materials are inherently multifunctional, as they also exhibit second-harmonic generation (SHG), piezoelectricity, and pyroelectricity. Molecular ferroelectrics are an alternative and emerging class of ferroelectrics, because they exhibit flexible molecular structures, optical transparency, low density, tunable physical and chemical properties and are synthesized using soft chemistry routes. The resulting molecular systems can exhibit electrical bistability above room temperature, making them competitive with perovskite type materials, as recently demonstrated for organo-ferroelectric materials based on croconic acid,[12] functionalized benzimidazoles,[13] bis(imadazolium)-L-tartrate,[14] and diisopropylammonium bromide.[15] Ferroelectric properties require the absence of an inversion center in the crystal structure that consequently gives rise to additional functionalities, such as non-linear optical properties or piezoelectricity. However, the combination of electrical bistability, luminescence, and magnetism in a single smart multifunctional molecule-based system has been rather scarce,[16] despite attractive applications, such as four-level density data storage or multifunctional sensors.[17]

[*] Dr. J. Long, J.-M. Thibaud, Dr. Y. Guari, Prof. Dr. J. Larionova
Institut Charles Gerhardt Montpellier
UMR 5253 CNRS-UM2-ENSCM-UM1
Equipe Ingénierie Moléculaire et Nano-Objets
Université Montpellier 2
Place Eugène Bataillon, 34095 Montpellier Cedex 5 (France)
E-mail: jerome.long@univ-montp2.fr

Dr. J. Rouquette, J.-M. Thibaud, Dr. J. Haines
Institut Charles Gerhardt Montpellier
UMR 5253 CNRS-UM2-ENSCM-UM1
Equipe Chimie et Cristallochimie des Matériaux
Université Montpellier 2
Place Eugène Bataillon, 34095 Montpellier Cedex 5 (France)

Dr. R. A. S. Ferreira, Prof. Dr. L. D. Carlos
Physics Department and CICECO, University of Aveiro
3810-193, Aveiro (Portugal)

B. Donnadieu
Fédération de Recherche Chimie Balard,-FR3105
Université Montpellier 2
Place Eugène Bataillon, 34095 Montpellier Cedex 5 (France)

V. Vieru, Prof. Dr. L. F. Chibotaru
Theory of Nanomaterials Group and INPAC
Katholieke Universiteit Leuven
Celesijnenlaan, 200F, Heverlee, B-3001 (Belgium)

Dr. L. Konczewicz
Laboratoire Charles Coulomb, UMR 5221
Université Montpellier 2
Place Eugène Bataillon, 34095 Montpellier Cedex 5 (France)

[**] We thank University Montpellier II and the CNRS for financial support. We also thank D. Granier (PAC Chimie Balard, Montpellier) for the single-crystal X-ray diffraction data. Fundação para a Ciência e a Tecnologia (FCT) and EU/FEDER COMPETE under contracts Pest-C/CTM/LA0011/2013 and FCOMP-01-0124-FEDER-037271 are also acknowledged.

Supporting information for this article is available on the WWW under http://dx.doi.org/10.1002/anie.201410523.

Herein, we report a rational approach to design multifunctional ferroelectric molecular materials by association of the Dy^{3+} ion with an enantiopure Zn^{2+}-Schiff base antenna complex in a non-centrosymetric crystal system. First, Dy^{3+} can exhibit luminescence with well-resolved emission bands and long lifetimes,[18] and the presence of the antenna coordination complex should enhance the lanthanide luminescence. Second, owing to the high magnitude doubly degenerate ground state ($\pm m_J$), Dy^{3+} possesses a large magnetic moment and a strong magnetic anisotropy, which is very attractive to design magnetic materials, including recently-emerging single-molecule magnets (SMM) and single-ion magnets (SIM).[19–21] Third, the chirality of the ligand may favor the crystallization of the whole molecular assembly in a non-centrosymetric space group compatible with ferroelectricity. Indeed, the ZnDy molecular material obtained behaves as a ferroelectric up to 563 K, the highest temperature reported for molecular ferroelectrics. It also exhibits Dy^{3+}-based luminescence, optical activity, and acts as a paramagnet at high temperature and as a SIM at low temperature. In this four-functional system, we investigate the correlations between the electric polarization and crystal structure and between the low temperature magnetic slow relaxation and the optical properties.

The stoechiometric reactions between either the enantiopure Schiff-base ligands *S*,*S*-H_2L or *R*,*R*-H_2L (H_2L = phenol, 2,2′[2,2-diphenyl-1,2-ethanediyl]bis[(*E*)-nitrilomethylidyne]-bis(6-methoxy) (Supporting Information, Scheme S1), $Zn(OAc)_2{\cdot}2H_2O$, and $Dy(NO_3)_3{\cdot}5H_2O$ in methanol yield, upon slow diffusion of diethyl ether, the formation of single crystals of [*R*,*R*-ZnLDy(μ-OAc)$(NO_3)_2$] (*R*,*R*-**1**) or [*S*,*S*-ZnLDy(μ-OAc)$(NO_3)_2$] (*S*,*S*-**2**), respectively. Single-crystal X-ray analysis performed at 173 K reveals that *R*,*R*-**1** and *S*,*S*-**2** are isostructural and crystallize in the polar space group $P2_1$ with the screw axis collinear to the *b* crystallographic axis (Supporting Information, Tables S1, S2). The crystallization in a polar space group highlights the efficient transfer of chirality from the ligand to the coordination complexes. Each enantiomer is composed of two crystallographically independent heterodinuclear complexes (Zn1A–Dy1A and Zn1B–Dy1B) in the asymmetric unit with closely related structures (Figure 1). In each complex, phenolate bridges ensure the connections between the Zn^{2+} and Dy^{3+} ions, leading to a Zn^{2+}–Dy^{3+} distance of 3.328(1) and 3.331(2) Å for Zn1A–Dy1A and Zn1B–Dy1B, respectively (Figure 1). The Zn^{2+} center is located in the inner compartment with the donor N_2O_2 set, while the hard Dy^{3+} ion is coordinated in the outer compartment through the O_2O_2 set. An acetate molecule bridges the two metallic centers and two bidentate nitrates complete the coordination sphere of the Dy^{3+} ion leading to a nonacoordinate environment. SHAPE analysis[22] (Supporting Information, Table S3, S4) reveals that both Dy1A and Dy1B adopt an intermediate geometry between a spherical capped square antiprism (C_{4v}) and a spherical tricapped trigonal prism (D_{3h}). The dinuclear complexes are well isolated in the crystal without any hydrogen bonds between the dinuclear units, the shortest Dy–Dy intermolecular distance being 9.21 Å (Figure 1).

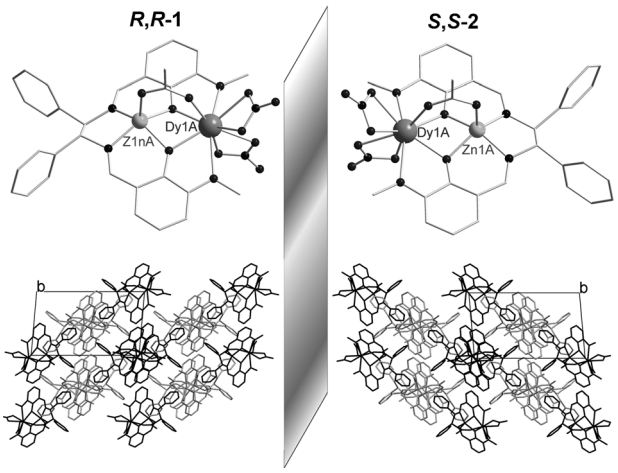

Figure 1. Top: Molecular structure of one of the dinuclear complexes *R*,*R*-**1** and *S*,*S*-**2**, showing their enantiomeric relationship. Bottom: View of the packing arrangement of the dinuclear complexes along the *b* crystallographic axis, emphasizing the two crystallographically independent complexes shown in black and gray.

Solid-state circular dichroism measurements performed at room temperature for *R*,*R*-**1** and *S*,*S*-**2** confirm their enantiomeric nature (Supporting Information, Figure S1). Each enantiomer exhibits mirror-symmetrical dichroism spectra with Cotton effects of opposite signs at $\lambda_{max} = 262$, 303, and 382 nm, confirming unambiguously the crystal structure refinement in the polar space group. Thermogravimetric analyzes (TGA) confirm the absence of solvent molecules in the lattice and indicate that *R*,*R*-**1** and *S*,*S*-**2** are perfectly stable up to 573 K (Supporting Information, Figure S2), while differential scanning calorimetry (DSC) analysis from 300 to 573 K indicates that no structural phase transition occurs up to the decomposition of the complex (Supporting Information, Figure S3). To further support this absence of structural phase transition, X-ray diffraction on a single crystal of *R*,*R*-**1** was performed in the 173–558 K temperature range. The data clearly show that the compound remains monoclinic with a polar space group ($P2_1$) over the investigated temperature range, with exceptionally good values for the refinement factor *R* and Flack parameter, confirming that no racemization occurs (Supporting Information, Tables S5–S9). Outstandingly, no disorder or significant thermal motion were found at high temperature and the quality of the X-ray data remained very high (Supporting Information, Figure S4).

Dielectric measurements were performed to further confirm the polar character of the complexes (Supporting Information, Figure S5). At ambient temperature, the dielectric constant ($\varepsilon'_r = 38$) is typical for molecular ferroelectrics, with a low dielectric loss[11] of 0.2 %, and dielectric susceptibility values start to diverge above 473 K. The absence of an anomaly in the dielectric susceptibility is in accordance with the results from X-ray diffraction and DSC. To study the ferroelectric behavior of the material, polarization measurements as a function of the applied electric field were performed up to 563 K on single crystals. At room temperature, the electric field required to efficiently polarize the material is too high to observe a hysteresis loop. At 400 K, the

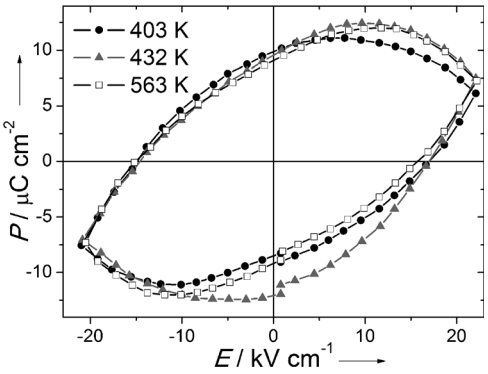

Figure 2. Dielectric hysteresis loop (1 Hz) for *R,R*-**1** obtained from a single crystal at different temperatures.

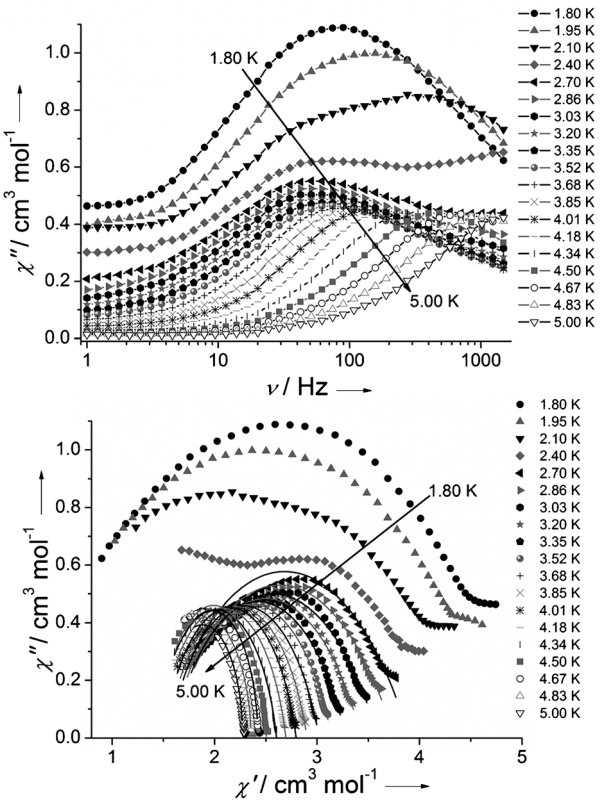

Figure 3. Top: Frequency dependence of the out-of-phase (χ'') susceptibility at different temperatures performed under a 1500 Oe DC field for *R,R*-**1**. Bottom: Cole–Cole (Argand) plot for *R,R*-**1** obtained using the ac susceptibility data (1500 Oe). The solid lines correspond to the best fit obtained with a generalized Debye model.

P vs. *E* curve (Figure 2) shows a clear hysteresis loop with a large coercitive field value of about 17 $kV\,cm^{-1}$ with a spontaneous polarization, P_S, of 9.1 $\mu C\,cm^{-2}$. This value is significantly higher than that of the archetypical ferroelectric Rochelle salt ($P_s = 0.25\ \mu C\,cm^{-2}$),[23] but is in the same order of magnitude in comparison with the values observed for several molecular ferroelectrics,[11] such as 2-methyl-benzimidazole ($P_s = 5.2\ \mu C\,cm^{-2}$)[12] or diisopropylammonium bromide ($P_s = 8.20\ \mu C\,cm^{-2}$) based materials.[15] However, our P_s and coercitive field values are most likely slightly overestimated owing to the contribution of leakage currents at these high temperatures (Supporting Information, Figure S6). Clear hysteresis loops are still observed at 563 K, 10 K before the decomposition of the complex. Even at such temperatures, fully saturated hysteresis cycles could not be obtained as a higher electric field would be required. These results indicate the compounds are ferroelectrics over the whole temperature range investigated. To the best of our knowledge, this is the highest temperature at which an electrical hysteresis loop is observed for a molecular ferroelectric. Moreover, this temperature is 170 K above of the Curie temperature of the archetypal ferroelectric $BaTiO_3$ and the spontaneous polarization is considerably greater.

The magnetic properties of *R,R*-**1** and *S,S*-**2** were investigated by using a SQUID magnetometer. The room temperature χT value of 13.44 $cm^3\,K\,mol^{-1}$ is in good agreement with the theoretical value of 14.17 $cm^3\,K\,mol^{-1}$ expected for one Dy^{3+} ion ($^6H_{15/2}$, $S = 5/2$, $L = 5$, $g = 4/3$). Upon cooling, χT decreases owing to the thermal depopulation of the Stark sublevels to 10.30 $cm^3\,K\,mol^{-1}$ at 1.8 K (Supporting Information, Figure S7). The field dependence of the magnetization at 1.8 K yields to a value of 5.57 μ_B at 7 T, which is close to the value observed for Dy^{3+} ions in comparable crystal fields.[10b]

AC measurements were performed to probe the evidence of a SIM behavior from individual complexes. Owing to the low symmetry of the dysprosium site and the presence of dipolar interactions, the fast quantum tunneling of the magnetization (QTM) precludes the observation of a slow relaxation at zero field. However, this phenomenon can be strongly reduced by applying a weak static magnetic field. Thus, an optimal DC field of 1500 Oe was determined from the variation of the maximum of the out-of-phase susceptibility χ'' as a function of the frequency (Supporting Information, Figures S8, S9). Frequency and temperature dependences of the ac susceptibilities (Figure 3; Supporting Information, Figures S10, S11) indicate the occurrence of two relaxation processes with a clear overlap which becomes evident when looking at the Cole–Cole plots (Figure 3). Fitting with a generalized Debye model leads to large value of the α parameter at low temperature (0.91 at 2.7 K), which strongly decreases to 0.20 at 4.6 K, indicating a moderate distribution of the relaxation time for the second relaxation process (Supporting Information, Table S10). By using the Arrhenius law, $\tau = \tau_0 \exp(U_{eff}/kT)$, the obtained parameters related to both relaxation processes are $U_{eff} = 19.40$ K (13.48 cm^{-1}) and $\tau_0 = 1.23 \times 10^{-8}$ s for the low-temperature relaxation and $U_{eff} = 51.82$ K (36.01 cm^{-1}) and $\tau_0 = 3.75 \times 10^{-9}$ s for the high-temperature relaxation (Supporting Information, Figure S12). A deviation from the purely thermally activated behavior appears for the lowest temperatures, indicating the existence of a quantum regime.

The parameters obtained for *SS*-**2** are $U_{eff} = 20.48$ K (14.23 cm^{-1}), $\tau_0 = 8.97 \times 10^{-9}$ s and $U_{eff} = 51.72$ K (35.93 cm^{-1}), $\tau_0 = 3.55 \times 10^{-9}$ s for the low- and high-temperature processes, respectively, and are close to what is obtained for *R,R*-**1** complex.

The occurrence of two different relaxation processes may be, at first glance, intuitively assigned to the presence of two crystallographically independent Dy^{3+} ions. However, the

almost identical crystal field environment of the lanthanide centers does not support such a scenario, and recently numerous examples of multiple relaxation processes with a crystallographically unique lanthanide ion have been reported.[24] For instance, the low-temperature relaxation processes can originate from direct relaxation process under a DC magnetic field.[25] This is indeed supported by ab initio calculations (Supporting Information, Table S11), which allow the estimation of the energies of the lowest Kramers doublets as well as the value of the g tensors for each crystallographic Dy^{3+} ion and for each enantiomer (Supporting Information, Tables S12 and S13). The large value of g_z (19.5) for the first Kramers doublet indicates that the ground Kramers doublet on each Dy^{3+} sites is close to $m_J = \pm 15/2$. The first excited Kramers doublet for each Dy^{3+} ion are found to be comparable for *R,R*-**1** (46 and 43 cm^{-1}) and are slightly higher than the effective energy barrier value obtained from ac magnetic data for the high-temperature process. In the case of *S,S*-**2**, a slight discrepancy between the energy first excited Kramers doublets is found with values of 64 and 43 cm^{-1}. On the other hand, the calculated transversal components of the g-factors for the ground Kramers doublet of DyA and DyB sites (g_x and g_y in the Supporting Information, Table S13) are relatively large compared to other complexes.[6c,9c,21b] These cause relatively large transversal Zeeman splittings of the corresponding Kramers doublets which induce QTM. The latter explains why the investigated compounds are not SIM without applied dc field (Supporting Information, Figure S8).

Given that Zn^{2+} complexes with Schiff bases are particularly appropriate to act as antennas to transfer energy towards Dy^{3+} ions, the photoluminescence properties of *R,R*-**1** and *S,S*-**2** were investigated in the solid state at room and at 12 K (Figure 4; Supporting Information, Figures S13–S17). At room temperature, both ligand (large band around 450 nm) and Dy^{3+} intra-4f^9 transitions can be observed owing to a partial energy transfer from the ligand to the lanthanide upon excitation at 365 nm. To provide further details on the Dy^{3+} coordination sphere, the photoluminescence features of both enantiomers were measured at 12 K. At this temperature, no sign of the ligand emission could be discerned, and only the Dy^{3+} $^4F_{9/2} \rightarrow {}^6H_{15/2-11/2}$ transitions could be detected, pointing out a more efficient energy transfer between the ligand-related states and the intra-4f levels. To correlate the magnetic and photoluminescence data, the low-temperature emission spectra of *R,R*-**1** and *S,S*-**2** compounds were further analyzed, using the same method that was recently reported.[10b,26] The presence of the two Dy^{3+}sites (A and B) makes it extremely difficult to fit unambiguously the $^4F_{9/2} \rightarrow {}^6H_{15/2}$ transition (with, at least, 16 Stark levels, assuming that only the $^4F_{9/2}$ low-energy component is populated). Therefore, we only analyzed the high-energy region (20900–21100 cm^{-1}) to estimate for both sites the energy difference between the ground level and the first $^6H_{15/2}$ Stark component U_A and U_B (Figure 4a,b). In this spectral range, the emission spectrum reveals the presence of four Stark components (two for each Dy^{3+} local site) ascribed to transitions from the first excited $^4F_{9/2}$ Stark sublevel to the two lowest Stark levels of the $^6H_{15/2}$ multiplet. Moreover, two hot bands arising from transitions from the first $^4F_{9/2}$ Stark sublevel (located at 40 cm^{-1} above the low-energy $^4F_{9/2}$ component)[10b] of each site to the corresponding ground level of the $^6H_{15/2}$ multiplet are also discerned (Figure 4b). Taking into account that relaxation of the magnetization occurs by an Orbach mechanism involving the first excited Kramers doublet, the separation between the levels of the two Dy^{3+} sites (labelled as A_1, A_2 and B_1, B_2, respectively) permits the zero-field energy barrier to be estimated, yielding to a value of $U_A = U_B = 40 \pm 3$ cm^{-1} for sites A and B. Similar values are obtained for *R,R*-**1**, as the emission spectra of the two enantiomers are almost coincident (Figure 4, top).

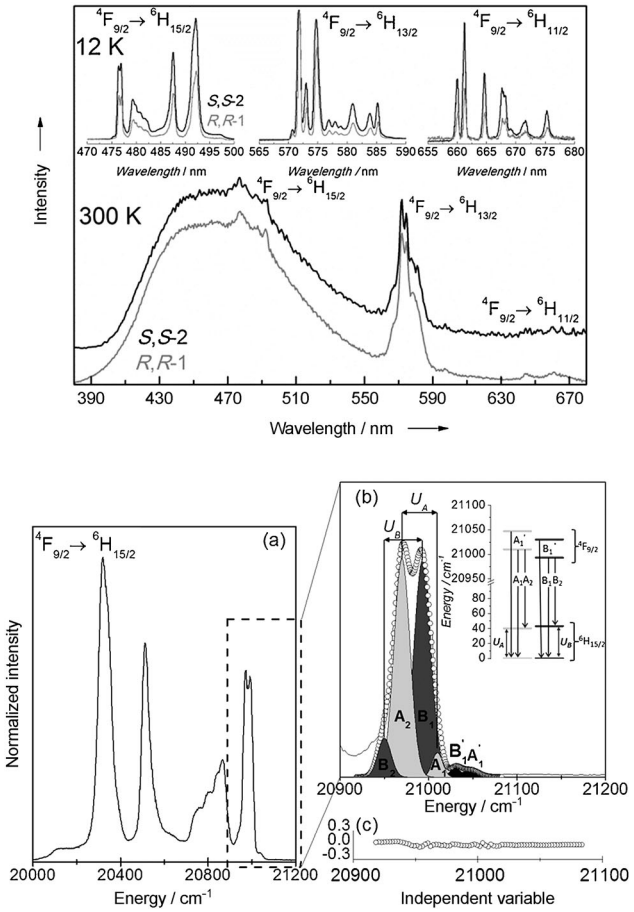

Figure 4. Top: Emission spectrum of *R,R*-**1** and *S,S*-**2** acquired at room temperature and at 12 K ($\lambda_{exc} = 365$ nm). Bottom: a) Magnification of the $^4F_{9/2} \rightarrow {}^6H_{15/2}$ transition for *S,S*-**2** at 12 K. b) Multi-Gaussian functions fit (○) and the components from the first $^4F_{9/2}$ Stark sublevels to the $^6H_{15/2}$ multiplet in the range 20900–21100 cm^{-1}. A_1' and B_1' denote hot bands arising from transitions from the first $^4F_{9/2}$ Stark sublevel to the ground level of the $^6H_{15/2}$ multiplet. c) Residual plot ($R^2 \approx 0.98$) for a judgment of the fit quality.

In summary, the design of molecular materials based on chiral lanthanide complexes appears as a powerful approach to rationally obtain high-temperature multifunctional molecular ferroelectrics with additional optical and magnetic properties. Thus, molecular crystals of *R,R*-**1** and *S,S*-**2** present an electrical bistability up to 563 K, the highest temperature reported for molecular ferroelectric materials. Remarkably, the structure remains polar with an exceptionally good crystallinity and an ordered structure up to the decomposition

of the complex around 570 K. This constitutes a striking example of a molecular material that can be competitive in terms of both properties and stability in comparison with metallic oxides.

Furthermore, this material exhibits optical activity, high- and low-temperature luminescence, and behaves as a paramagnet at high temperature (with a large magnetic moment) and a superparamagnet at low temperature yielding a tetrafunctional system that can be the ideal candidate for further investigations of coupling or synergetic effects between the constitutive functionalities. Thus, magneto-electrical effects can be expected, or modification of the emission spectrum by applying a magnetic and/or an electric field. These results definitely open new perspectives such as a four-level data-storage system based on a single molecule at low temperature that could be detected on a surface by its emission spectrum.

Received: October 28, 2014
Published online: December 30, 2014

Keywords: chirality · lanthanides · luminescence · molecular ferroelectrics · single-ion magnets

[1] E. Coronado, A. Forment-Aliago, J. R. Galan-Mascaros, C. Gimenez-Saiz, C. J. Gomez-Garcia, E. Martinez-Ferrero, A. Nuez, F. Romero, *Solid State Sci.* **2003**, *5*, 917.
[2] L. Ouahab, *Multifunctional Molecular Materials*, Pan Stanford Publishing, Pte Ltd,Singapore, **2013**.
[3] S. Chorazy, R. Podgany, W. Nitek, T. Fic, E. Görlich, M. Rams, B. Sieklucka, *Chem. Commun.* **2013**, *49*, 6731.
[4] C. Train, T. Nuida, R. Gheorghe, M. Gruselle, S.-I. Ohkoshi, *J. Am. Chem. Soc.* **2009**, *131*, 16838.
[5] P. Dechambenoit, J. R. Long, *Chem. Soc. Rev.* **2011**, *40*, 3249.
[6] a) C. Train, R. Gheorghe, V. Krstic, L.-M. Chamoreau, N. S. Ovanesyan, G. L. J. A. Rikken, M. Gruselle, M. Verdaguer, *Nat. Mater.* **2009**, *7*, 729; b) C. Train, M. Gruselle, M. Verdaguer, *Chem. Soc. Rev.* **2011**, *40*, 3297; c) G. Novitchi, G. Pilet, L. Ungur, V. V. Moshchalkov, W. Wernsdorfer, L. F. Chibotaru, D. Luneau, A. K. Powell, *Chem. Sci.* **2012**, *3*, 1169.
[7] E. Coronado, P. Day, *Chem. Rev.* **2004**, *104*, 5419.
[8] a) E. Chelebaeva, J. Larionova, Y. Guari, R. A. S. Ferreira, L. D. Carlos, F. A. Almeida Paz, A. Trifonv, C. Guérin, *Inorg. Chem.* **2008**, *47*, 775; b) E. Chelebaeva, J. Long, J. Larionova, R. A. S. Ferreira, L. D. Carlos, F. A. Almeida Paz, J. B. R. Gomes, A. Trifonov, C. Guérin, Y. Guari, *Inorg. Chem.* **2012**, *51*, 9005.
[9] a) S.-I. Ohkoshi, H. Tokoro, T. Matsuda, H. Takahashi, H. Irie, K. Hashomoto, *Angew. Chem. Int. Ed.* **2007**, *46*, 3238; *Angew. Chem.* **2007**, *119*, 3302; b) E. Pardo, C. Train, H. Liu, L.-M. Chamoreau, B. Dkhil, K. Boubekeur, F. Lloret, K. Nakatani, H. Tokor, S.-I. Ohkoshi, M. Verdaguer, *Angew. Chem. Int. Ed.* **2012**, *51*, 8356; *Angew. Chem.* **2012**, *124*, 8481; c) Y. X. Wang, W. Shi, H. Li, Y. Song, L. Fang, Y. H. Lan, A. K. Powell, W. Wernsdorfer, L. Ungur, L. F. Chibotaru, M. R. Shen, P. Cheng, *Chem. Sci.* **2012**, *3*, 3366.
[10] a) G. Cucinotta, M. Perfetti, J. Luzon, M. Etienne, P.-E. Car, A. Caneschi, G. Galvez, K. Bernot, R. Sessoli, *Angew. Chem. Int. Ed.* **2012**, *51*, 1606; *Angew. Chem.* **2012**, *124*, 1638; b) J. Long, R. Vallat, R. A. S. Ferreira, L. D. Carlos, F. A. Almeida Paz, Y. Guari, J. Larionova, *Chem. Commun.* **2012**, *48*, 9974; c) F. Pointillart, B. Le Guennic, S. Golhen, O. Cador, O. Maury, L. Ouahab, *Chem. Commun.* **2013**, *49*, 615.
[11] a) W. Zhang, H.-Y. Ye, R.-G. Xiong, *Coord. Chem. Rev.* **2009**, *253*, 2980; b) M. Guo, H.-L. Cai, R.-G. Xiong, *Inorg. Chem. Commun.* **2010**, *13*, 1590; c) T. Hang, W. Zhang, H.-Y. Ye, R. G. Xiong, *Chem. Soc. Rev.* **2011**, *40*, 3577.
[12] S. Horiuchi, Y. Tokunaga, G. Giovannatti, S. Picozzi, H. Itoh, R. Shimano, R. Kumai, Y. Tokura, *Nature* **2010**, *463*, 789.
[13] S. Horiuchi, F. Kagawa, K. Hatahara, K. Kobayashi, R. Kumai, Y. Murakami, Y. Tokura, *Nat. Commun.* **2012**, *3*, 1308.
[14] a) Z. Sun, T. Chen, J. Luo, M. Hong, *Angew. Chem. Int. Ed.* **2012**, *51*, 3871; *Angew. Chem.* **2012**, *124*, 3937; b) M. Szafrański, *Angew. Chem. Int. Ed.* **2013**, *52*, 7076; *Angew. Chem.* **2013**, *125*, 7214.
[15] D.-W. Fu, H.-L. Cai, Y. Liu, Q. Ye, W. Zhang, Y. Zhang, X.-Y. Chen, G. Giovannetti, M. Capone, J. Li, R.-G. Xiong, *Science* **2013**, *339*, 425.
[16] a) P.-H. Guo, J.-L. Liu, J.-H. Jia, J. Wang, F.-S. Guo, Y.-C. Chen, W.-Q. Lin, J.-D. Leng, D.-H. Bao, X.-D. Zhang, J.-H. Luo, M.-L. Tong, *Chem. Eur. J.* **2013**, *19*, 8769; b) X.-L. Li, C.-L. Chen, H.-P. Xiao, A.-L. Wang, C.-M. Liu, X. Zheng, L.-J. Gao, X.-G. Yang, S.-M. Fang, *Dalton Trans.* **2013**, *42*, 15317; c) P.-H. Guo, Y. Meng, Y.-C. Chen, Q.-W. Li, B.-Y. Wang, J.-D. Leng, D.-H. Bao, J.-H. Jia, M.-L. Tong, *J. Mater. Chem. C.* **2014**, *2*, 8858.
[17] a) M. Gajek, M. Bibes, S. Fusil, K. Bouzehouane, J. Fontcuberta, A. Bartherlemy, *Nat. Mater.* **2007**, *6*, 296; b) J. F. Scott, *Nat. Mater.* **2007**, *6*, 256.
[18] J.-C. Bünzli, C. Piguet, *Chem. Soc. Rev.* **2005**, *34*, 1048, and references therein.
[19] J. D. Rinehart, J. R. Long, *Chem. Sci.* **2011**, *2*, 2078.
[20] D. N. Woodruff, R. E. P. Winpenny, R. A. Layfield, *Chem. Rev.* **2013**, *113*, 5110.
[21] a) P.-H. Lin, T. J. Burchell, R. Clérac, M. Murugesu, *Angew. Chem. Int. Ed.* **2008**, *47*, 8848; *Angew. Chem.* **2008**, *120*, 8980; b) L. F. Chibotaru, L. Ungur, A. Soncini, *Angew. Chem. Int. Ed.* **2008**, *47*, 4126; *Angew. Chem.* **2008**, *120*, 4194; c) C. Aronica, G. Pilet, G. Chastanet, W. Wernsdorfer, J.-F. Jacquot, D. Luneau, *Angew. Chem. Int. Ed.* **2006**, *45*, 4659; *Angew. Chem.* **2006**, *118*, 4775; d) R. A. Layfield, J. J. W. McDouall, S. A. Sulway, F. Tuna, D. Collison, R. E. P. Winpenny, *Chem. Eur. J.* **2010**, *16*, 4442; e) J. Long, F. Habib, P.-H. Lin, I. Korobkov, G. Enright, L. Ungur, W. Wernsdorfer, L. F. Chibotaru, M. Murugesu, *J. Am. Chem. Soc.* **2011**, *133*, 5319.
[22] D. Casanova, M. Llunel, P. Alemany, S. Alvarez, *Chem. Eur. J.* **2005**, *11*, 1479.
[23] J. Vakasek, *Phys. Rev.* **1921**, *17*, 475.
[24] a) P. E. Car, M. Perfetti, M. Mannini, A. Favre, A. Caneschi, R. Sessoli, *Chem. Commun.* **2011**, *47*, 3751; b) M. Jeletic, P.-H. Lin, J. J. Le Roy, I. Korobkov, S. I. Gorelsky, M. Murugesu, *J. Am. Chem. Soc.* **2011**, *133*, 19286; c) J. Ruiz, A. J. Mota, A. Rodriguez-Diéguez, S. Titos, J.-M. Herrera, E. Ruiz, E. Cremandes, J.-P. Costes, E. Colacio, *Chem. Commun.* **2012**, *48*, 7916.
[25] M. M. Hänninen, A. J. Mota, D. Aravena, E. Ruiz, R. Sillanpää, A. Camon, M. Evangelisti, E. Colacio, *Chem. Eur. J.* **2014**, *20*, 8410.
[26] M. Ren, S.-S. Bao, R. A. S. Ferreira, L.-M. Zheng, L. D. Carlos, *Chem. Commun.* **2014**, *50*, 7621.

